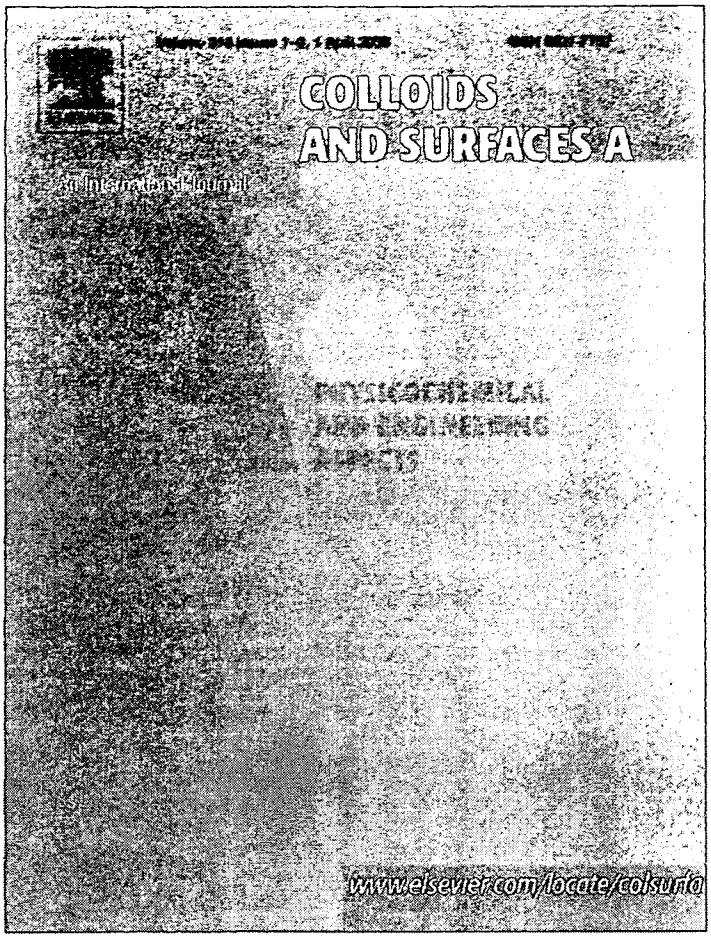

Available online at www.sciencedirect.com
ScienceDirect
Colloids and Surfaces A: Physicochem. Eng. Aspects 318 (2008) 184–190
COLLOIDS AND SURFACES A
www.elsevier.com/locate/colsurfa

Fabrication of free-standing nanoparticle-fused nanosheets and their hetero-modification using sacrificial film

Yosuke Okamura[a], Saori Utsunomiya[a], Hidenori Suzuki[b], Daisuke Niwa[c], Tetsuya Osaka[c], Shinji Takeoka[c,*]

[a] *Graduate School of Advanced Science and Engineering, Waseda University, Tokyo 169-8555, Japan*
[b] *Center for Electron Microscopy, The Tokyo Metropolitan Institute of Medical Science, Tokyo 113-8613, Japan*
[c] *Consolidated Research Institute for Advanced Science and Medical Care, Waseda University, Tokyo 169-8555, Japan*

Received 11 September 2007; received in revised form 11 December 2007; accepted 19 December 2007
Available online 6 January 2008

Abstract

Sheet-shaped carriers, having obverse and reverse surfaces and thus a large contact area as a targeting site, have several advantages over spherical-shaped carriers, which have an extremely small contact area. Herein is proposed a novel method for the preparation of free-standing nanoparticle-fused nanosheets having uniform micrometer shape, nanometer thickness and heterogenous surfaces, using a water-soluble sacrificial film. This was achieved by combination of four processes: (1) specific adsorption of latex beads at pH 5.0 and a concentration of 1.0×10^{11} mL^{-1} onto a patterned dodecyltrimethoxysilane self-assembled monolayer (DTS-SAM) region by a conventional dry patterning process, (2) fabrication of the latex bead-sheet via thermal-fusion at 110 °C for 60 s, (3) preparation of the free-standing nanosheet by detachment from the DTS-SAM, and (4) hetero-modification of the resulting nanosheet using a water-soluble poly(acrylic acid) as a sacrificial supporting film. Thus, this sheet-shaped carrier having hetero-surfaces can be regarded as a new material for delivery of drugs, hemostatic reagents and as wound dressings for burn injury, etc.

Keywords: Free-standing; Nanosheet; Thermal fusion; Sacrificial film; Hetero-modification

1. Introduction

In recent years, much attention has been paid to drug delivery systems (DDS) as a new pharmacological approach for improving the efficacy and safety of drugs. In DDS, vesicles, micelles, emulsions, and biodegradable nanoparticles have been extensively studied as carriers for biologically active substances such as drugs, recognition proteins, enzymes, genes, etc. [1]. There are two concepts for the development of DDS, passive and active targeting systems. In the latter case, recognition proteins such as antibodies and various ligands are conjugated to the surface of the carriers to target tissue epitopes or specific cells.

The present group has developed biocompatible and biodegradable nanoparticles such as albumin-based nanoparticles [2,3] and phospholipid vesicles [4,5] carrying recombinant fragments of platelet membrane proteins [2,4] and fibrinogen dodecapeptide as a recognition site for activated GPIIb/IIIa on the platelet surface [3,5]. These nanoparticles specifically recognize the site of a bleeding injury or activated platelets. In this approach to the conjugation of high or low molecular weight molecules such as glycoprotein Ibα and dodecapeptide to the surface of the particle, it was observed that the activity of the peptide was suppressed by steric hindrance of the large protein; therefore, a spacer such as a poly(ethylene glycol) chain was found to be necessary to conjugate the peptide [6].

On the other hand, sheet-shaped carriers, having obverse and reverse surfaces and thus a large contact area as a targeting site, have several advantages over spherical-shaped carriers, which have a relatively small contact area. Recently, several approaches have been implemented for fabrication of free-standing films, combining a large surface area with

* Corresponding author at: Consolidated Research Institute for Advanced Science and Medical Care, Waseda University, 3-4-1, 65-208 Ohkubo Shinjuku-ku, Tokyo 169-8555, Japan. Tel.: +81 3 5286 3217; fax: +81 3 5286 3217.
E-mail address: takeoka@waseda.jp (S. Takeoka).

0927-7757/$ – see front matter © 2007 Elsevier B.V. All rights reserved.
doi:10.1016/j.colsurfa.2007.12.049

nanoscale thickness. These approaches have included the use of polymers and/or inorganic materials such as cast films [7], layer-by-layer (LbL) films of polyelectrolytes [8–10], cross-linked amphiphilic Langmuir–Blodgett films [11], self-assembled monolayers (SAMs) [12] and assemblies of triblock copolymers [13].

Organosilane SAMs have been widely used in applications designed to change physical and chemical properties of the surface of glass, quartz, SiO_2/Si wafers, or silica particles [14]. Furthermore, they are excellent tools for immobilization of proteins such as redox proteins [15], enzymes [16] and immunogloblins via covalent or non-covalent bond formation; ionic or hydrogen bonding, van der Waals attraction, or hydrophobic interaction occurs with various terminal groups of SAMs. It is generally easy to construct patterned SAMs with uniform size and shape on silicon oxide using conventional photolithography processes [17]. The present group recently proposed a novel method for preparation of free-standing biocompatible nanosheets derived from recombinant human serum albumin (rHSA) molecules adsorbed on patterned hydrophobic SAMs [18].

Two-dimensional patterns with steady repeatability in the particle array have been achieved by site-selective deposition using chemical bonding or electrostatic interaction [19], an electrophotography method [20], a micromold method and gravity [21], a micromold method and a lateral capillary force [22], a patterned Au film and a drying process of colloidal solution onto the patterned Au film [23], an excellent method of HSA-supported lipid patterns by using a micro-contact printing technique to immobilize microspheres and *E. coli* [24,25]. Furthermore, a novel method for deposition of a close-packed particle monolayer onto a patterned hydrophilic SAM was also recently reported using a liquid mold whose drying process was also described [26,27]. However, there is no report on the preparation of free-standing nanoparticle-based nanosheets having uniform micrometer shape, nanometer thickness and heterogenous surfaces, for use as sheet-shaped carriers.

Herein is proposed a novel method for the preparation of a free-standing nanoparticle-based nanosheet with uniform shape and thickness, incorporating hetero-modification of the obverse and reverse surfaces using a poly(acrylic acid) (PAA) film as a sacrificial layer. A patterned hydrophobic dodecyltrimethoxysilane SAM (DTS-SAM) on silicon oxide was used to prepare the nanosheets. Furthermore, latex beads were used as model particles with high monodispersibility, and fluorescent dyes were used to modify the surface of the sheet and to prove the hetero-modification of the nanosheet by staining the sheet surfaces.

2. Materials and methods

2.1. Reagents

P-type Si (1 0 0) wafers (below 0.02 Ω cm) covered with thermally grown silicon oxide (approximately 200 nm), were purchased from KST World, Co. (Fukui). *n*-Dodecyltrimethoxysilane (DTS, 97%) was purchased from Gelest, Inc. (Morrisville, PA). Latex beads (Polybead™, Ø100 nm) were purchased from Polysciences, Inc. (Warrington, PA). Fluorescein-4-isothiocyanate (FITC) and 5,(6)-tetramethylrhodamine isothiocyanate (TRITC) were purchased from Dojindo Laboratories, Inc. (Kumamoto) and Invitrogen, Co. (Carlsbad, CA), respectively. Poly(acrylic acid) (Mw = 450,000) and 0.1% (w/v) poly-L-lysine solution were obtained from Sigma–Aldrich Co. (Saint Louis, MO). A microBCA kit was purchased from Pierce Biotechnology, Inc. (Rockford, IL). Recombinant human serum albumin (rHSA, 250 mg mL^{-1}) was kindly donated by Oxgenix Co. Ltd. (Tokyo).

2.2. SAM preparation

Silicon wafers were treated with SPM (96% H_2SO_4:30% H_2O_2 = 4:1 (v/v)) at 120 °C followed by rinsing with distilled water. The resulting wafers were placed in a 20-mL teflon vial containing a glass cup filled with 200 μL DTS liquid. The vials were sealed with a cap and then heated for 8 h at a constant temperature of 110 °C in a dry room to prepare a hydrophobic DTS-SAM on the silicon oxide [28].

2.3. Patterning processes

The patterned DTS-SAM with hydrophobic dodecyl regions and hydrophilic silicon oxide regions on the substrate were prepared by a conventional photolithography process. The DTS-SAM on the silicon oxide was covered with photoresist (OFPR-800 500 cP, Tokyo Ohka Kogyo, Co. Ltd., Kanagawa), and was irradiated with a 350-nm UV lamp (MA-10, Mikasa Ltd., Tokyo) using a photomask (size: 1 cm × 1 cm, patterning; rectangle (5 μm × 10 μm), Topic Co., Ltd., Saitama). After developing (NMD-3), the substrate was exposed to oxygen plasma (Plasma Reactor PR301, Yamato Scientific Co. Ltd., Tokyo) at an input power of 200 W and an oxygen flow rate of 80 sccm for removal of DTS. The photoresist was removed by acetone washing to obtain a patterned DTS-SAM.

2.4. Contact angle measurements

A 3-μL drop of distilled water was placed directly onto the DTS-SAM with a micro-pipette before and after adsorption of latex beads at pH 5.0, or after the addition of surfactant as described below. The liquid drops were observed with an optical microscope with 5× magnification. All water contact angles were represented as the mean ± standard deviation of five measurements.

2.5. Measurement of the glass transition temperature of the latex beads

The glass transition temperature (T_g) of the latex beads was measured by differential scanning calorimetry (DSC, Thermo plus DSC 8230, Rigaku Co., Osaka). The analysis was performed with approximately 10 mg of freeze-dried sample under a dynamic nitrogen atmosphere with a heating rate of 10 °C min^{-1}.

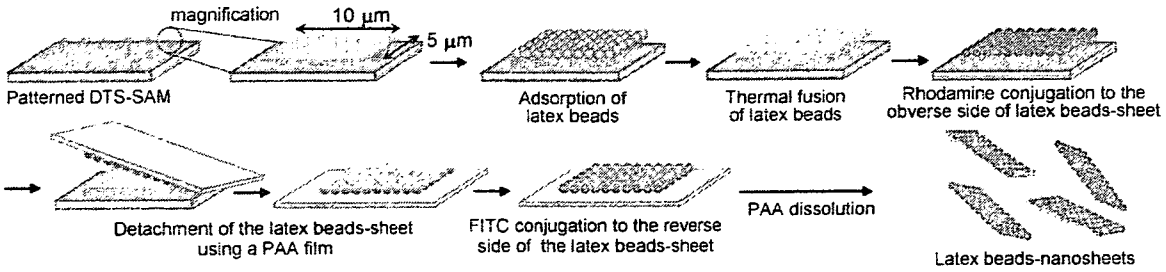

Fig. 1. Preparation of free-standing latex bead-fused sheets having hetero-surfaces using the patterned DTS-SAM.

2.6. Preparation of free-standing latex bead-fused nanosheets

Latex beads (Ø100 nm) were mixed with an rHSA solution (20 mg mL^{-1}) and incubated at r.t. for 2 h to coat the surface of the latex beads with rHSA. After separation of the free rHSA by ultracentrifugation (100,000 × *g*, 10 min, 4 °C, twice), the rHSA-coated latex beads (rHSA-latex beads, 5.0×10^{12} mL^{-1}) were dispersed into a phosphate buffer solution (pH 7.4). The amount of rHSA adsorbed on the surface of the latex beads was analyzed with a microBCA kit.

As shown in Fig. 1, the substrate of the patterned DTS-SAM was immersed in an acetate buffer suspension (pH 5.0) of the rHSA-latex beads at a concentration of 1.0×10^{11} mL^{-1}. After withdrawing the substrate from the suspension, the remaining suspension on the substrate was slowly blown off with a horizontal stream of N_2 in order to adsorb the latex beads onto the hydrophobic dodecyl patterned region, after which the substrate was immediately washed with distilled water. The series of adsorption and washing procedures of latex beads on the substrate was repeated 10 times in order to obtain a closely packed pattern of latex beads. After drying the substrate under a N_2 flow, the substrate was heated at 110 °C for 60 s to thermally fuse the adsorbed latex beads. Poly(acrylic acid) was dissolved in distilled water (20 mg mL^{-1}) to prepare a PAA solution, the PAA cast on the substrate and dried at r.t. for 15 h to make a supporting film. After peeling off the resulting PAA film, it was dissolved in a phosphate buffer solution at pH 7.4 to obtain free-standing latex bead-fused nanosheets. The resulting nanosheets were observed with a Hitachi S-4500 field emission scanning electron microscope (SEM) as follows: the nanosheets adsorbed on a silicon substrate and the free-standing nanosheets collected on the membrane filter (pore size 0.4 μm, Nuclepore®, Whatman, Inc., Clifton, NJ) were coated with osmium tetroxide (ca. 5-nm thick) using an osmium plasma coater (NL-OPC80, Nippon Laser & Electronics Lab., Nagoya), and were observed at an accelerating voltage of 8 kV. In the case of the PAA film, to which the latex bead-fused nanosheets were transferred, the accelerating voltage was set at 1 kV.

2.7. Hetero-modification of the latex bead-fused nanosheets

In this study, a large-scale substrate with the patterned DTS-SAM, established using a photomask (size: 4 cm × 4 cm, patterning; rectangle (5 μm × 10 μm)) was used. As shown in Fig. 1, following thermal treatment the substrate was immersed in a solution of 5-μM TRITC in phosphate buffer (pH 7.4), and incubated at r.t. for 5 min. The unreacted TRITC was removed with distilled water, and the TRITC-labeled nanosheet on the substrate was collected. Next, a PAA solution was cast on the substrate and dried at r.t. for 15 h. After peeling off the PAA film from the substrate, a 5-μM FITC solution in a phthalate buffer (pH 4.0, saturated with sodium chloride) was added to the reverse side of the resulting PAA film to which the TRITC-labeled latex bead-fused sheet had been transferred, and incubated at r.t. for 5 min. Finally, the PAA film was dissolved with a phosphate buffer (pH 7.4) and the fluorescent-labeled nanosheets were then collected and washed with distilled water by centrifugation (1000 × *g*, 5 min, r.t.).

Next, a glass plate (24 mm × 60 mm, thickness 0.12–0.17 mm) was immersed in a poly-L-lysine solution at r.t. for 1 h, and then carefully rinsed with phosphate buffer. The nanosheets was applied to the resulting poly-L-lysine-coated glass plate and incubated at r.t. for 1 h. The resulting nanosheets were observed with a confocal laser scanning microscope (LSM 510, Zeiss, Nikon Co., Tokyo).

3. Results and discussion

3.1. Characterization of the rHSA-latex beads

Latex beads were coated with rHSA molecules to stabilize their dispersion states, to avoid non-specific binding of the latex beads to the substrate, and to be able to conjugate various molecules to the amino groups of rHSA. The quantity of rHSA coating the surface of the latex beads at a concentration of 1.0×10^{11} mL^{-1} was determined to be 14.2 μg mL^{-1} by a microBCA method, from which the number of rHSA molecules on one latex bead (approximate diameter 100 nm) was estimated to be approximately 1.2×10^3 molecules. The theoretical number was calculated to be approximately 1.2×10^3 molecules, assuming that rHSA molecules (the average surface area of one rHSA molecule being 25.5 nm^2) [29] were closely packed on the surface of a latex bead of 100-nm diameter (surface area: 3.1×10^4 nm^2). Consequently, it was possible to estimate the surface of latex beads fully coated with rHSA molecules.

3.2. Water contact angle

The hydrophobic dodecyltrimethoxysilane (DTS), which has a terminal CH_3 group, was selected as a raw material for the

Table 1
Water contact angles of DTS-SAM before and after rHSA-latex beads adsorption

rHSA-latex beads adsorption	Water contact angle (°)
Before	83 ± 1
After	73 ± 3
[a]$C_{12}E_{10}$	82 ± 6

[a] $C_{12}E_{10}$ was added to the DTS-SAM after rHSA-latex beads adsorption and incubated at r.t. for 1 h, and then washed with distilled water.

SAM. The water contact angle of the DTS-SAM-coated substrate was estimated to be 83 ± 1° as shown in Table 1, whereas the contact angle of the silicon oxide surface before DTS coating was estimated to be 20 ± 2°. This supported the conclusion that the hydrophobic DTS-SAM was successfully coated on the silicon oxide surface. When the DTS-SAM-coated substrate was immersed in a dispersion of the rHSA-latex beads in acetate buffer (pH 5.0), the water contact angle was significantly decreased to 73 ± 3°, suggesting that the rHSA-latex beads were adsorbed on the DTS-SAM. When the substrate treated with the rHSA-latex beads was immersed in a 1% (v/v) solution of $C_{12}E_{10}$ for 1 h, the contact angle returned to 82 ± 6° (i.e. the same as that of the DTS-SAM substrate before treatment with the rHSA-latex beads). This indicated that the rHSA-latex beads were adsorbed on the DTS-SAM by hydrophobic interaction and detached by surfactant treatment.

3.3. Specific adsorption of the latex beads and their thermal fusion

A conventional dry patterning process was adopted for the specified adsorption of the rHSA-latex beads onto the patterned DTS-SAM as follows. When the dispersion of the latex beads (1.0×10^{11} mL^{-1}, pH 5.0) was applied to the substrate and the suspension remaining on the substrate was then slowly blown off with a horizontal stream of N_2 gas, the latex beads were arranged as a monolayer on the entire substrate, regardless of hydrophobic and hydrophilic regions (data not shown). It is possible that assembling of the latex beads would involve nucleation initiated by a capillary force and growth driven by a laminar flow to evaporate water; after this the particles might be forced to arrange in the form of a monolayer as previously reported [30].

Next, immediate and repeated washing of the substrate with an acetate buffer (pH 5.0) detached the rHSA-latex beads from the hydrophilic SiO_2 region and beads remained on the rectangular patterns of the hydrophobic dodecyl region only (5 μm × 10 μm). Considering the results obtained from the water contact angle experiment, this indicated that the rHSA-latex beads were firmly adsorbed onto the patterned DTS-SAM by hydrophobic interaction. This would occur because the net charge of the rHSA-latex beads at pH 5.0, near the isoelectric point of rHSA, would be approximately zero. On the other hand, it was assumed that the rHSA-latex beads were easily detached from the SiO_2 region because they were only weakly attracted by hydrophobic interaction with the hydrophilic SiO_2 region (where the ζ-potential of the SiO_2 region at pH 5.0 was extremely negative, ca. −50 mV) [31]. Finally, after repeating the adsorption of the latex beads on the substrate plus washing 10 times, the rHSA-latex beads were closely packed in a monolayer pattern as shown in Fig. 2(A) and (B). On the other hand, at pH 7.4, the rHSA-latex beads were also adsorbed on the entire substrate. After washing, the latex beads were easy to detach from the hydrophilic SiO_2 region and were then scattered on the rectangular patterns of the hydrophobic dodecyl region. This suggested

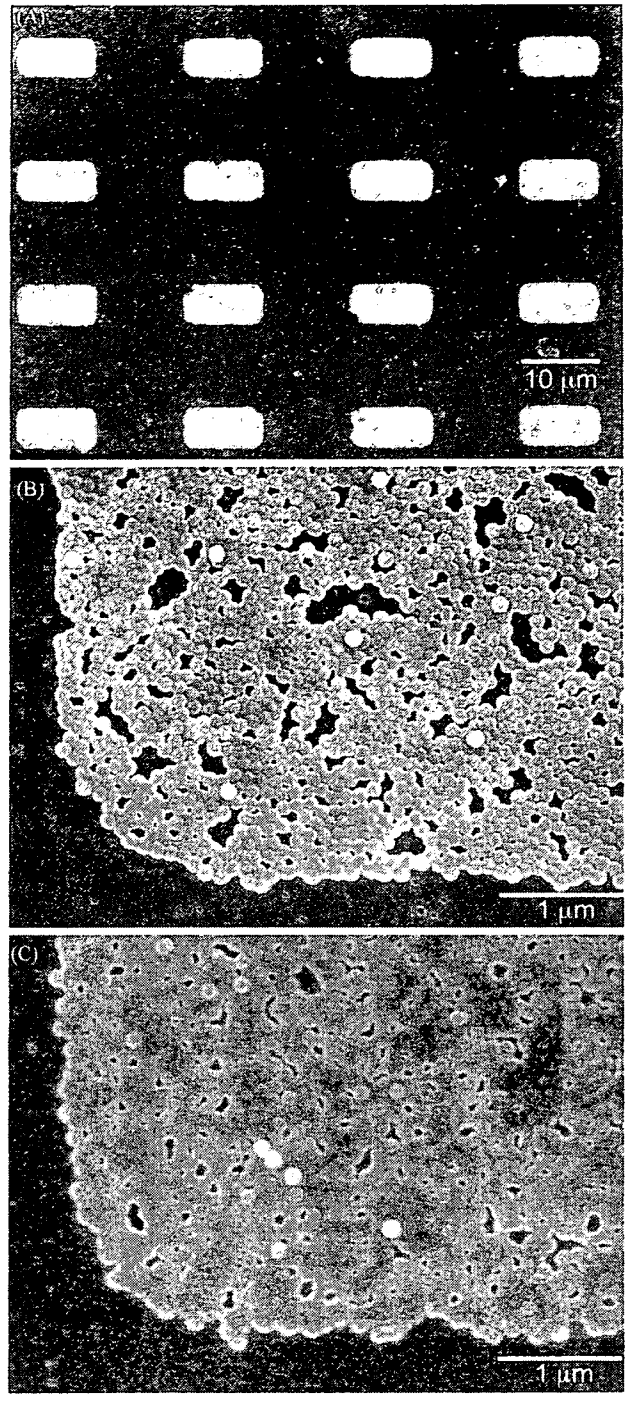

Fig. 2. (A) SEM image of rHSA-latex beads specifically adsorbed onto the patterned DTS-SAM. Magnified SEM image of rHSA-latex beads adsorbed onto the patterned DTS-SAM (B) before and (C) after thermal fusion.

that the rHSA-latex beads, which are negatively charged at pH 7.4, were electrostatically repelled from each other when the particles were arranged by the capillary force of a dry process.

The glass transition temperature of the freeze-dried latex beads was next determined by a DSC measurement in order to thermally fuse the rHSA-latex beads adsorbed on the patterned DTS-SAM; T_g was 109.9 °C. The latex bead-adsorbed substrate was heated at 110 °C for 60 s with a hotplate after drying with N_2. Though the surface of the resulting sheet maintained the spherical configuration of the constituent latex beads, the neighboring latex beads were sufficiently fused under these conditions as shown in Fig. 2(C). When the latex bead-fused nanosheet was detached from the DTS-SAM using a PAA film as described below, it was confirmed that the reverse side of the nanosheet, which was directly adsorbed on the DTS-SAM, was flat and smooth (data not shown). This suggested that it was possible to distinguish the obverse and reverse sides of the nanosheets after detachment. Heating at 110 °C for 30 s, did not yield a sufficiently fused nanosheet. On the other hand, heating for over 120 s resulted in melting and spreading outwards of the latex beads adsorbed on the patterned DTS-SAM (data not shown).

3.4. Preparation of free-standing latex bead-fused nanosheets

PAA was used as a water-soluble sacrificial film to disperse the latex bead-fused sheets. The PAA solution was cast on the substrate where the nanosheets had been adsorbed and dried at r.t. for 15 h. It was easy to peel off the PAA film from the substrate and the resulting film was tough and clear as shown in Fig. 3(A). Observation of the PAA film using an SEM confirmed that the latex bead-fused nanosheet was completely transferred to the PAA film as shown in Fig. 3(B), and no residual sheets were observed on the substrate (data not shown). Such complete transfer is possible because the ionic and/or hydrogen bonding between the PAA and the latex bead-fused nanosheets would be stronger than the van der Waals interaction of the dried nanosheets with the CH_3-terminal SAMs. In agreement with the report by Stroock et al., describing the exquisite transfer of a polymer film on a substrate to a PAA film and suspension in an aqueous buffer, their transfer mechanism has been successfully reproduced in the patterned nanosheets [32]. Furthermore, it was easy to dissolve the resulting PAA film to release the latex bead-fused nanosheet in a phosphate buffer at pH 7.4, and the free-standing nanosheets were collected on the membrane filter as shown in Fig. 3(C). It was confirmed that these nanosheets were able to maintain their rectangular shape, indicating in turn that the neighboring latex beads were sufficiently well fused to retain the two-dimensional shape. Furthermore, it was judged that the thickness of the nanosheets was approximately 100 nm because the latex beads were arranged in a monolayer as shown in Fig. 2(A) and (B).

Detachment of the nanosheets from the substrate was also attempted using other methods. For example, application of sonication for a few minutes caused the latex bead-fused nanosheets to break into pieces although they were dispersed from the substrate. Addition of the surfactant ($C_{12}E_{10}$) was ineffective in detaching nanosheets from the substrate, even by immersion in a 1% $C_{12}E_{10}$ solution for several hours; however, the non-fused latex beads could be simply detached. This suggested that $C_{12}E_{10}$ molecules did not diffuse into the spaces between the nanosheets and the DTS-SAM substrate because (i) the

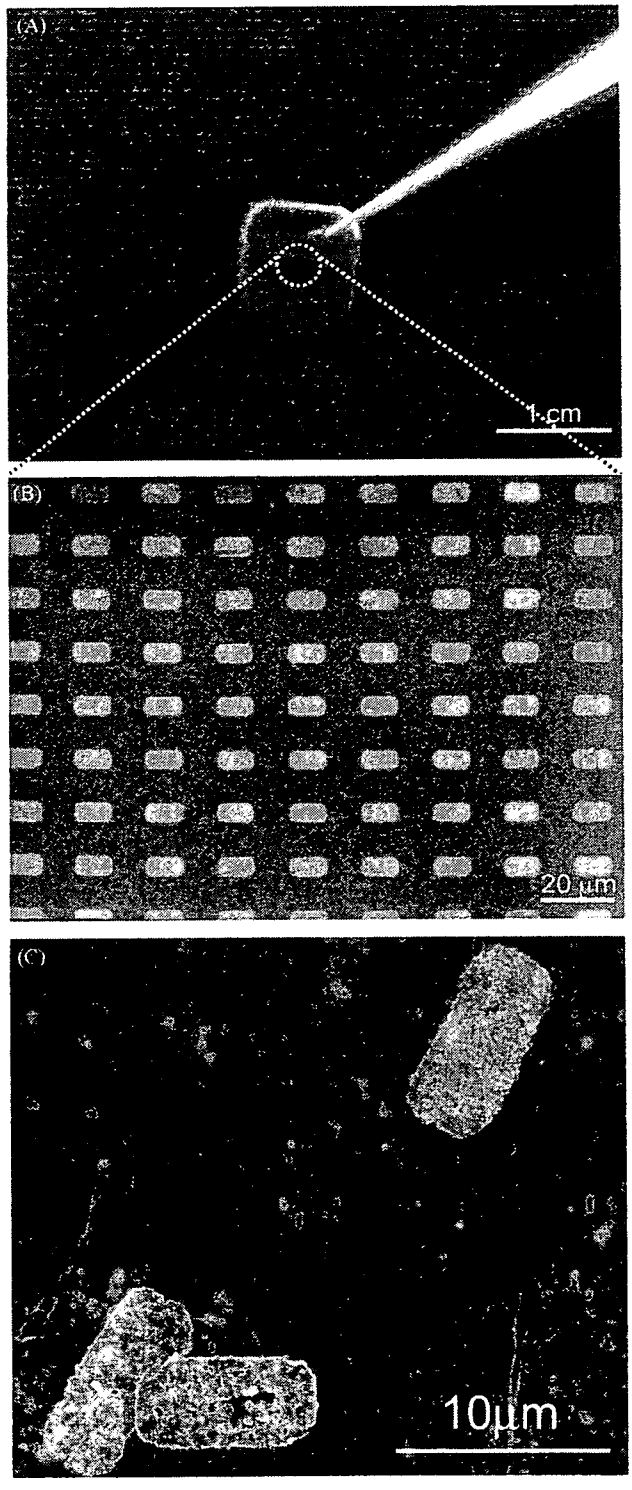

Fig. 3. (A) Photo and (B) SEM image of latex bead-fused nanosheets transferred from the DTS-SAM to the PAA film. (C) SEM image of free-standing latex bead-fused sheets after dissolution of the resulting PAA film.

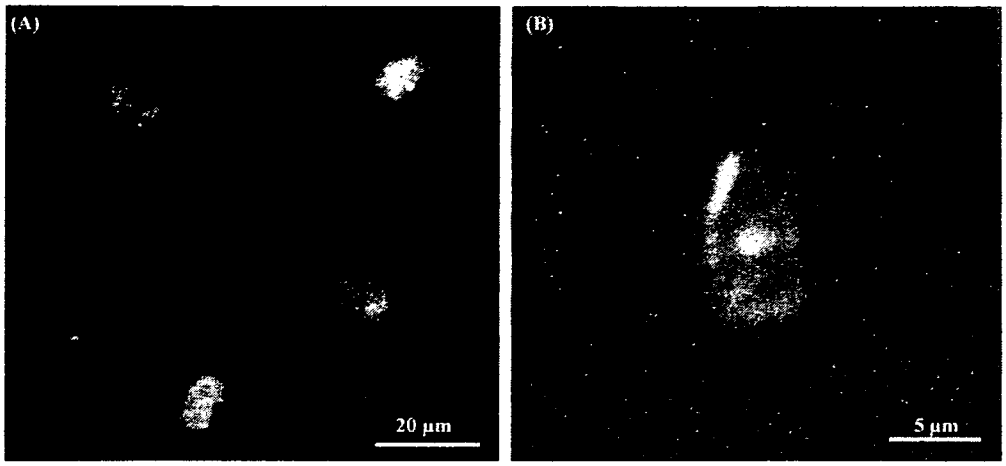

Fig. 4. (A) Images of TRITC and FITC-labeled latex bead-fused sheets and (B) magnified image of the latex bead-fused nanosheets using confocal laser fluorescence microscopy.

nanosheet was interacting two-dimensionally with DTS-SAM and (ii) the hydrophobic bonding of the nanosheet was stronger than that of non-fused latex beads. In summary therefore, it has been confirmed that transference of the nanosheets to the PAA film was an excellent method to achieve dispersion of the nanosheets into an aqueous solution.

3.5. Hetero-modification of the latex bead-fused nanosheet

When the PAA film supporting the latex bead-fused nanosheets was observed, it was easy to confirm that the reverse smooth side of the nanosheet, which had been in direct contact with the silicon substrate, emerged onto the surface of the resulting PAA film (data not shown). It is concluded that either side of the nanosheet could be selectively modified using the PAA film, not only as a tool for transference of the sheets and a sacrificial film for dispersion, but also as a supporting film for hetero-modification of the nanosheet.

Two kinds of water-soluble fluorescent probes, TRITC and FITC were selected as model components to show hetero-modification of the nanosheet. An excess of TRITC (5 μM) was firstly added to the amino groups of the rHSA-adsorbing latex beads on the patterned DTS-SAM. After sufficient washing with distilled water, the PAA solution was cast on the substrate and the dried PAA film was peeled off. For FITC modification of the reverse side of the nanosheets, conditions under which the PAA film would be insoluble were used: pH 4.0 and saturated sodium chloride. An excess of FITC (5 μM) was added to the reverse side of the PAA film which was then dissolved in a phosphate buffer at pH 7.4, to allow collection of latex bead-fused nanosheets coated with each of the two fluorescent labels. Using a confocal laser scanning microscope, the abundance of rectangular nanosheets was confirmed as shown in Fig. 4(A), on one or other of the two surfaces where either fluorescent probe was localized: the obverse side of the nanosheets was conjugated with TRITC and the reverse side was conjugated with FITC (Fig. 4(A) and (B)). Thus, this study has proved that the latex bead-fused sheet was able to modify selectively either surface using the PAA film as a supporting film.

4. Conclusions

Preparation of free-standing rectangular (5 μm × 10 μm) nanoparticle-fused sheets has been successfully achieved by thermal fusion on the patterned DTS-SAM. Also, hetero-modification of the nanosheets on both surfaces has been achieved using the PAA film as a supporting film for hetero-modification. Experimental strategies under development involve preparation of biocompatible and biodegradable free-standing sheet-shaped carriers for drug delivery, delivery of hemostatic reagents and wound dressings for burn injury, etc.

Acknowledgments

This work was supported by 21COE "Practical Nano-Chemistry", "Consolidated Research Institute for Advanced Science and Medical Care" from MEXT, Japan, and Shorai Foundation for Science and Technology (S.T.). Y.O. was the recipient of a Research Fellowships from the Japan Health Science Foundation.

References

[1] Y. Tomii, Lipid formation as a drug carrier for drug delivery, Curr. Pharm. Design 8 (2002) 467–474.
[2] Y. Teramura, Y. Okamura, S. Takeoka, H. Tsuchiyama, H. Narumi, M. Kainoh, M. Handa, Y. Ikeda, E. Tsuchida, Hemostatic effects of polymerized albumin particles bearing rGPIa/IIa in thrombocytopenic mice, Biochem. Biophys. Res. Commun. 306 (2003) 256–260.
[3] Y. Okamura, S. Takeoka, Y. Teramura, Y. Maruyama, E. Tsuchida, M. Handa, Y. Ikeda, Hemostatic effects of fibrinogen γ-chain dodecapeptide-conjugated polymerized albumin particles in vitro and in vivo, Transfusion 45 (2005) 1221–1228.
[4] S. Takeoka, Y. Teramura, Y. Okamura, E. Tsuchida, M. Handa, Y. Ikeda, Rolling properties of rGPIbα-conjugated phospholipid vesicles with different membrane flexibilities on vWf surface under flow conditions, Biochem. Biophys. Res. Commun. 296 (2002) 765–770.
[5] Y. Okamura, I. Maekawa, Y. Teramura, Y. Maruyama, E. Tsuchida, M. Handa, Y. Ikeda, S. Takeoka, Hemostatic effects of phospholipid vesicles carrying fibrinogen γ-chain dodecapeptide in vitro and in vivo, Bioconjug. Chem. 16 (2005) 1589–1596.

[6] Y. Okamura, M. Handa, H. Suzuki, Y. Ikeda, S. Takeoka, New strategy of platelet substitutes for enhancing platelet aggregation at high shear rates; cooperative effects of a mixed system of fibrinogen γ-chain dodecapeptide- or glycoprotein Ibα-conjugated latex beads under flow conditions, J. Artif. Organs 9 (2006) 251–258.
[7] J. Mattson, J.A. Forrest, L. Borjesson, Quantifying glass transition behaviour in ultrathin free-standing polymer films, Phys. Rev. E 62 (2000) 5187–5200.
[8] Z. Tang, N.A. Kotov, S. Magonov, B. Ozturk, Nanostructured artificial nacre, Nat. Mater. 2 (2003) 413–418.
[9] F. Mallwitz, A. Laschewsky, Direct access to stable, freestanding polymer membranes by layer-by-layer assembly of polyelectrolytes, Adv. Mater. 17 (2005) 1296–1299.
[10] A. Mamedov, N. Kotov, Free-standing layer-by-layer assembled films of magnetite nanoparticles, Langumuir 16 (2000) 5530–5533.
[11] F. Mallwitz, W.A. Goedel, Physically cross-linked ultrathin elastomeric membranes, Angew. Chem. Int. Ed. 40 (2001) 2645–2647.
[12] W. Eck, A. Küller, M. Grunze, B. Völkel, A. Gölzhäuser, Freestanding nanosheets from crosslinked biphenyl self-assembled monolayers, Adv. Mater. 17 (2005) 2583–2587.
[13] C. Nardin, M. Winterhalter, W. Meier, Giant free-standing ABA triblock copolymer membranes, Langumuir 16 (2000) 7708–7712.
[14] A. Ulman, An Introduction to Ultrathin Organic Films from Langmuir–Blodgett to Self-assembly, Academic Press, San Diego, CA, 1991.
[15] D.E. Khoshtariya, J. Wei, H. Liu, H. Yue, D.H. Waldeck, Charge-transfer mechanism for cytochrome *c* adsorbed on nanometer thick films. Distinguishing frictional control from conformational gating, J. Am. Chem. Soc. 125 (2003) 7704–7714.
[16] E.E. Ferapontova, S. Shipovskov, L. Gorton, Bioelectrocatalytic detection of theophylline at theophylline oxidase electrodes, Biosens. Bioelectron. 22 (2007) 2508–2511.
[17] D. Niwa, Y. Yamada, T. Homma, T. Osaka, Formation of molecular templates for fabricating on-chip biosensing devices, J. Phys. Chem. B 108 (2004) 3240–3245.
[18] Y. Okamura, T. Goto, D. Niwa, M. Otsuka, N. Motohashi, T. Osaka, S. Takeoka, Fabrication of free-standing albumin-nanosheets having hetero-surfaces, J. Biomed. Mater. Res. A (2008), in press.
[19] Y. Masuda, W.S. Seo, K. Koumoto, Arrangement of nanosized ceramic particles on self-assembled monolayers, Jpn. J. Appl. Phys. 39 (2000) 4596–4600.
[20] H. Fudouzi, M. Kobayashi, M. Egashira, N. Shinya, An arrangement of micrometer-sized powder particles by electron beam drawing, Adv. Powder Technol. 8 (1997) 251–262.
[21] W.J. Wen, N. Wang, D.W. Zheng, C. Chen, K.N. Tu, Two- and three-dimensional arrays of magnetic microspheres, J. Mater. Res. 14 (1999) 1186–1189.
[22] Y. Sun, G.C. Walker, Two-dimensional self-assembly of latex particles in wetting films on patterned polymer, J. Phys. Chem. B 106 (2002) 2217–2223.
[23] Q. Guo, C. Arnoux, R.E. Palmer, Guided assembly of colloidal particles on patterned substrates, Langmuir 17 (2001) 7150–7155.
[24] X. Zhang, Q. He, Y. Cui, L. Duan, J. Li, Human serum albumin supported lipid patterns for the targeted recognition of microspheres coated by membrane based on ss-DNA hybridization, Biochem. Biophys. Res. Commun. 349 (2006) 920–924.
[25] X. Zhang, Q. He, X. Yan, P. Boullanger, J. Li, Glycolipid patterns supported by human serum albumin for *E. coli* recognition, Biochem. Biophys. Res. Commun. 358 (2007) 424–428.
[26] Y. Masuda, K. Tomimoto, K. Koumoto, Two-dimensional self-assembly of spherical particles using a liquid mold and its drying process, Langmuir 19 (2003) 5179–5183.
[27] Y. Masuda, K. Koumoto, Low dimensional particle patterning, J. Disper. Sci. Technol. 25 (2004) 503–511.
[28] H. Sugimura, H. Ushiyama, A. Hozumi, O. Takai, Micropatterning of alkyl- and fluoroalkylsilane self-assembled monolayers using vacuum ultraviolet light, Langmuir 16 (2000) 885–888.
[29] D.C. Carter, J.X. Ho, Structure of serum albumin, Adv. Protein. Chem. 45 (1994) 153–204.
[30] N.D. Denkov, O.D. Velev, P.A. Kralchevsky, I.B. Ivanov, H. Yoshimura, K. Nagayama, Mechanism of formation of two-dimensional crystals from latex particles on substrates, Langmuir 8 (1992) 3183–3190.
[31] A. Hozumi, S. Asakura, A. Fuwa, N. Shirahata, T. Kameyama, Preparation of a well-defined amino-terminated self-assembled monolayer and copper microlines on a polyamide substrate covered with an oxide nanoskin, Langmuir 21 (2005) 8234–8242.
[32] A.D. Stroock, R.S. Kane, M. Weck, S.J. Metallo, G.M. Whitesides, Synthesis of free-standing quasi-two-dimensional polymers, Langmuir 19 (2003) 2466–2472.

第34巻第4号平成20年4月25日発行（毎月1回25日発行）　昭和54年8月27日第3種郵便物認可　ISSN 1347-4340

Medical Science Digest

MSD 4

Vol.34
No.4
2008
通巻437号

メディカル・サイエンス・ダイジェスト（「組織培養工学」改題）

特集 インクレチンMimetica

—基礎と臨床—

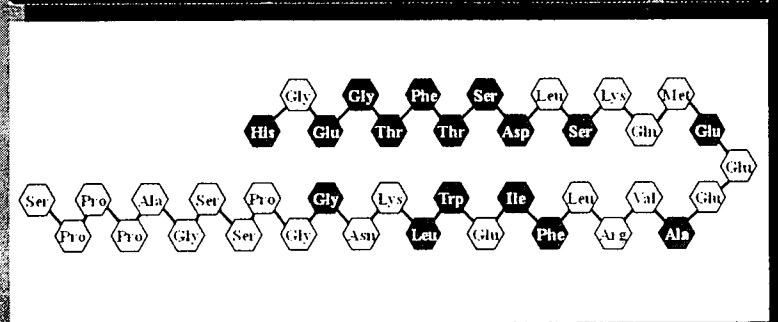

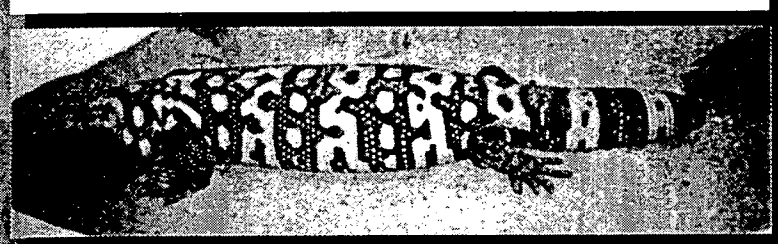

特集編輯　清野　裕
（関西電力病院　院長）

ニューサイエンス社

New Technology

人工血小板の開発

Development of Artificial Platelets

岡村 陽介[1,2]・武岡 真司[1]・半田 誠[2]・池田 康夫[3]

Key Words: Artificial platelet, polymerized albumin particle, phospholipid vesicle, rGPIbα, rGPIa/IIa, fibrinogen γ-chain dodecapeptide (H12)

Abstract

血小板は，血液凝固系と連動した巧妙な止血機構を有しており，これらすべてを具備した人工系の構築は不可能といっても過言ではない。我々は，血小板が出血部位において認識して粘着，凝集する分子機構に着目し，その主要な分子(GPIbα，GPIa/IIa，フィブリノーゲン由来アミノ酸配列(H12)など)を担持させた静注可能な人工微粒子(アルブミン重合体やリン脂質小胞体)を設計し，特異的に出血部位へ集積させ，活性化血小板と共に充填させることにより止血効果を期待した。本報ではその評価結果を報告する。

■はじめに

医療の進歩に伴い，癌・造血器腫瘍などの化学治療や放射線治療が年々増加する一方で，その副作用により血小板減少患者が増大している。血小板輸血は，化学治療，放射線治療，あるいは外科手術において不可欠な補助治療法として重要な位置を占めており，その供給量は年々増加し続け，平成11年以降は一定推移を保っている[1]。しかし，血小板製剤の保存期間は室温で4日間と非常に短いため，慢性的な供給不足に加えて緊急時の供給体制は整っていない。

更に，核酸増幅検査(NAT)の導入により血液製剤の安全性は著しく向上したものの，未だにウィルス感染などのリスクは完全には払拭されていない。従って，人工血小板の開発並びに臨床応用は，21世紀に於ける医療において当然目指すべき方向と思われる。

■止血機序と人工血小板の設計

止血の初期段階は，血管損傷部位に露出している血管内皮下組織への血小板の粘着と凝集である。高血流状態では，血小板膜糖蛋白質Ib(GPIb)がフォンビレブランド因子(VWF)を介したコラーゲンとの相互作用によって血小板の接着(ローリング)が起こる。続いて，低血流状態でコラーゲンの受容体蛋白質であるGPIa/IIaやGPVIがコラーゲンと直接結合して強固な粘着が起こる。接着，粘着の刺激が細胞内シグナルとして伝達されGPIIb/IIIaの高次構造が変化し(活性化)，血漿蛋白質であるフィブリノーゲンやVWFを介した血小板凝集が起こる。同時に，血小板内の濃染顆粒が開放小管系と膜融合してアデノシン5'-二リン酸(ADP)，Ca^{2+}，セロトニンが放出され，血小板間，あるいは白血球をも巻き込んだネットワークを形成して血小板凝集(一次止血)を促す。最後にトロンボキサンA_2の放出や血小板表面が凝固系の活性に必要な場(ホスファチジルセリン)として提供され，凝固因子カスケード反応が活性化されてフィブリン塊(血餅)となって止血(二次止血)が完了する。

このように血小板による止血には，巧妙に制御された多段階の反応が連動しているため，この機能を全て模倣した人工系の構築は不可能である。我々は，血小板が出血部位を認識して粘着，凝集する分子機構に着目し，血管損傷部位や血小板表面を認識できる分子を微粒子表面に担持させれば，これが出血部位へ特異的に集積して血栓形成を誘

Yosuke Okamura[1,2], Shinji Takeoka[1], Makoto Handa[2], and Yasuo Ikeda[3]
[1] 早稲田大学先進理工学部生命医科学科[2] 慶應義塾大学医学部輸血・細胞療法部[3] 慶應義塾大学医学部内科
[1] Department of Life Science and Medical Bioscience, School of Advanced Science and Engineering, Waseda University.[2] Department of Transfusion Medicine & Cell Therapy, School of Medicine, Keio University.
[3] Department of Internal Medicine, School of Medicine, Keio University.

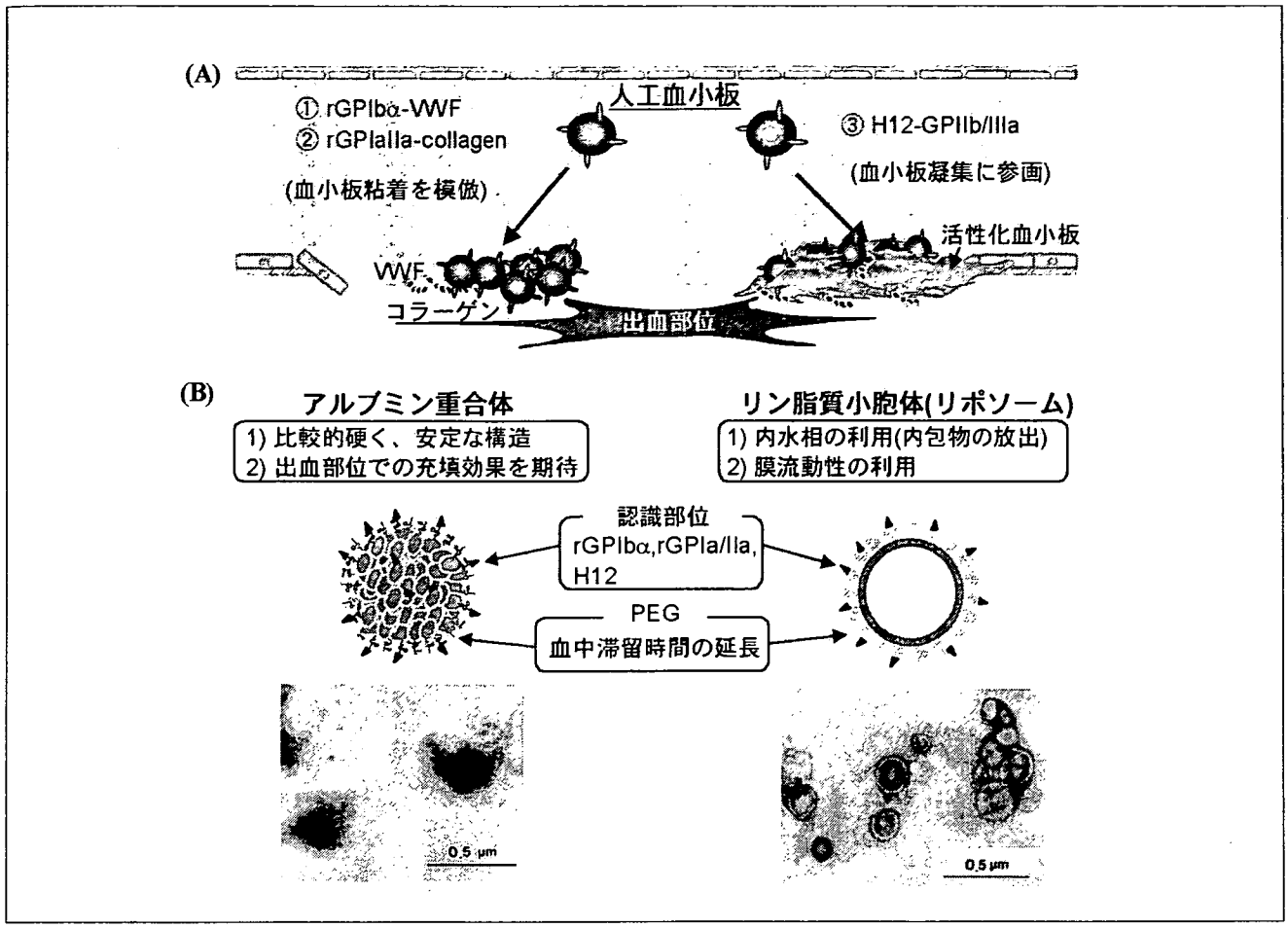

図　人工血小板の概念図

(A) 血小板の接着，粘着に関与する血小板膜蛋白質rGPIbα, rGPIa/IIa，血小板凝集に参画するフィブリノーゲン由来ドデカペプチド(H12)を微粒子表面に結合させることで出血部位へ特異的に集積させ，出血部位の充填効果が期待できる。
(B) 人工血小板用の担体として開発したアルブミン重合体とリン脂質小胞体の特徴と電子顕微鏡像。

導する起点となり，出血部位を充填して止血効果が期待できるとの発想から，極めて単純な人工血小板の設計に結びつけた（図(A)）。具体的には，静注可能な遺伝子組換えヒト血清アルブミン(rHSA)の重合体やリン脂質小胞体(リポソーム)を微粒子として利用し，出血部位を認識させるために血小板膜糖蛋白質の一部の遺伝子組換え蛋白質(rGPIbα，rGPIa/IIa)やフィブリノーゲンγ鎖C末端アミノ酸配列(HHLGGAKQAGDV: H12)を担持させた系を構築して*in vitro*，*in vivo*評価を行っている。

■微粒子の製造方法と機能評価

我々は，rHSAを単量体とし，そのpHと温度の制御のみでジスルフィド重合させるクリーンかつ簡便なアルブミン重合体の調製法を確立している[2]。重合度の制御によりナノからマイクロスケールの粒径制御が可能であり，アルブミン重合体は内部が充填された無定形な形態をとっている（図(B)）。他方，リン脂質を水中に分散させると自発的に集合して多重層小胞体が構築される。これを孔径の異なるメンブレンに順次透過させると，粒子径と膜層数の制御が可能となる。さらに，小胞体表面へ種々の蛋白質を担持させて特定部位への指向性，集積性が期待できる（図(B)）。

小胞体やアルブミン重合体の表面にrGPIbαやrGPIa/IIaを結合させると，血小板の接着(ローリング)，粘着現象が再現できる[3]。興味深いことにそのローリング速度は，小胞体を構成する二分子膜の柔軟性と相関しており，“柔らかい”小胞体ではローリング速度は低下し，“硬い”小胞体では上昇した。これは“柔らかい”小胞体は変形しやすくVWF基板と小胞体間の接触面積が増大したために

ローリング速度が低下したためと考えられる。ところが，アルブミン重合体ではVWF表面をローリングせずに粘着する。従って，ローリングには流動性のある膜構造が必要と思われた。

他方，アルブミン重合体や小胞体にフィブリノーゲンγ鎖C末端ドデカペプチド(HHLGGAKQAGDV, H12)を結合させると，血小板凝集促進機能が発現する[4, 5]。具体的には，血小板減少モデル血液(2.0×10^4 /μL，正常の10分の1)にH12結合アルブミン重合体を添加し，コラーゲン基板に対する血小板の粘着挙動を流動下で観察したところ，その未添加系と比較して血小板の粘着を約2倍も増大させた。さらに，抗がん剤(ブスルファン)をWister系雄性ラットに20 mg/kgにて投与すると，その副作用によって，投与10日後に血小板数のみが正常の5分の1まで再現性よく減少した[4]。血小板減少症モデルラットの尾先端から1cmの箇所をクイックヒール®にて切傷後，生理食塩水に浸して出血時間を測定すると，再現性良く計測できた(608±152秒，正常ラット: 178±56秒)。そこで，H12結合アルブミン重合体を投与すると出血時間が投与量依存的に有意に短縮された(288±120秒)[4]。

また，血中滞留時間の延長を目的としてアルブミン重合体の表面をポリエチレングリコール鎖にて修飾し，その末端の一部にH12を結合した系では，投与6時間後でもその止血効果が持続することも確認できている。また，担体を小胞体に置き換えても，同様の止血効果が得られている[5]。しかし，この両者を同一粒子数を投与した群同士で比較した場合，アルブミン重合体の方がその効果は優れているようである。これは，アルブミン重合体は内部が充填されているため，出血部位の充填効果が高いためと推測できる。しかし，小胞体ならば内水相に血小板の活性化や凝固系を誘導する因子を内包可能であり，出血部位に集積した小胞体がこれらを放出することにより，より効果的に出血時間を短縮する系の構築も可能になりつつある(未発表データ)。

■今後の展開と課題

血小板減少動物モデルを用いた止血効果に関する知見も次々に集積され，我々の人工血小板の設計方針の正当性が立証でき，人工血小板の実用化の可能性が見えてきた。今後は，臨床試験に向けてその適応を明確にした上で，より大型動物(ウサギ，霊長類)を用いた効能試験や安全性試験(血液生化学試験，毒性試験)を行う必要がある。将来，バイオテクノロジーやオプトエレクトロニクスの進歩により血小板の動的機能に関する多くの情報が短期間に蓄積され，同時に遺伝子組換え蛋白質の大量製造や担体の製剤化技術の飛躍が期待できるため，我々の研究成果は人工血小板の開発のみならずDrug Delivery Systemの基盤技術の発展にも繋がるものと期待される。

文　献

1) 日本赤十字社ホームページ　http://www.jrc.or.jp/active/blood/index.html.
2) Takeoka S *et al.*: Biomacromolecules. 1: 427-462, 2000.
3) Takeoka S *et al.*: Biochem. Biophys. Res. Commun. 296: 765-770, 2002.
4) Okamura Y *et al.*: Transfusion. 45: 1221-1228, 2005.
5) Okamura Y *et al.*: Bioconjugate Chem. 16: 1589-1596, 2005.

News (学会情報)

第112回　日本眼科学会総会

テーマ：そして未来へ。
会　期：2008年4月17日（木）～20日（日）
会　場：パシフィコ横浜　http://www.pacifico.co.jp/
招待講演　4月19日（土）10:50～11:50　第1会場（メインホール）
2）バイオマテリアルと生体組織工学とを駆使した先端医療の最前線
座 長：吉村　長久　京都大学
演 者：田畑　泰彦　京都大学・再生医科学研究所生体組織工学研究部門　生体材料学分野
●第112回 日本眼科学会総会 運営事務局（株式会社コングレ内）
〒102-8481 東京都千代田区麹町5-1 弘済会館ビル　TEL：03-5216-5551　FAX：03-5216-5552

Revised Manuscript for Journal of Biomedical Material Research Part A

Fabrication of Free-standing Albumin-Nanosheets Having Hetero-Surfaces

Yosuke Okamura, Takahiro Goto, Daisuke Niwa, Yoshihito Fukui, Masanobu Otsuka, Norikazu Motohashi, Tetsuya Osaka and Shinji Takeoka[§]

(Received:)

Consolidated Research Institute for Advanced Science and Medical Care, Waseda University, Tokyo, 169-8555, Japan.

[§] To whom correspondence should be addressed.
e-mail: takeoka@waseda.jp, Tel: +813-5286-3217, Fax: +813-5286-3217

ACKNOWLEDGMENTS

This work was partly supported by Shorai Foundation for Science and Technology (S.T.). Y.O. was the recipient of a Research Fellowships from the JSPS for Young Scientists and the recipient of Japan Health Sciences Foundation.

ABSTRACT

Sheet-shaped carriers, having both obverse and reverse surfaces and thus a large contact area for targeting a site, have several advantages over spherical shaped carriers, which have an extremely small contact area for targeting sites. Here, we proposed a novel method to prepare a free-standing ultra-thin and biocompatible nanosheet having hetero-surfaces, by a combination of four processes; [1] specific adsorption of recombinant human serum albumin (rHSA) molecules onto a patterned octadecyltrimethoxysilane self-assembled monolayer region (ODS-SAM), [2] preparation of nanosheets of rHSA molecules bearing thiol groups (SH-rHSA) via two-dimensionally disulfide cross-linking, [3] surface modification of the resulting nanosheet, [4] preparation of the free-standing nanosheet by detachment from the ODS-SAM. The SH-rHSA molecules at pH 5.0 and a concentration of 1 μg/mL were specifically adsorbed on the patterned ODS-SAM regions by hydrophobic interaction, and were two-dimensionally cross-linked in the presence of copper ion as an oxidant. The rHSA-nanosheets were then simply detached from the ODS-SAM by treatment with surfactant. We succeeded in the preparation of rectangular (10 x 30 μm) and ultra-thin (4.5 ± 1.0 nm) rHSA-nanosheets on a patterned ODS-SAM, and could also obtain free-standing rHSA-nanosheets having hetero-surfaces by surface modification with fluorescent latex beads. Thus, the rHSA-nanosheets having hetero-surfaces could be regarded as a new biomaterial for drug carriers, hemostatic reagents and wound dressing for burn injury etc..

KEY WORDS

albumin, nanosheet, free-standing, biocompatibility, cross-kinking

INTRODUCTION

In recent years, much attention has been paid to drug delivery systems (DDS) as a new pharmacological approach, to improve the efficacy and safety of drugs. In DDS, vesicles, micelles, emulsions, and biodegradable nanoparticles have been extensively studied as carriers for biologically active substances such as drugs, recognition proteins, enzymes, genes, etc. (1). There are two concepts for the development of DDS, passive and active targeting

systems. In the latter case, recognition proteins such as antibodies and various ligands are conjugated to the surface of the carriers to target the tissue epitopes or specific cells.

We have developed biocompatible and biodegradable nanoparticles such as albumin-based nanoparticles (2-5) and phospholipid vesicles (6, 7) carrying recombinant fragments of platelet membrane proteins (3, 4, 6, 8) and dodecapeptide as a recognition site for fibrinogen (2, 5, 7, 9). These nanoparticles specifically recognized the site of bleeding injury or activated platelets. In our approach to the conjugation of high and low molecular weight molecules such as glycoprotein Ibα and dodecapeptide to the surface of the particle, we observed that the activity of dodecapeptide was suppressed by the steric hindrance of the glycoprotein Ibα, and found that a spacer such as a poly(ethylene glycol) chain was needed in the conjugation of the peptides (8).

On the other hand, sheet-shaped carriers, having both obverse and reverse surfaces and thus a large contact area for targeting a site, have several advantages over spherical shaped carriers, which have an extremely small contact area for targeting sites. Recently, several approaches have been implemented for the fabrication of free-standing films, combining large surface area with nanoscale thickness, from polymers and/or from inorganic materials; cast films (10), layer-by-layer (LbL) assemblies of polyelectolyte multilayers (11-15), cross-linked amphiphilic Langmuir-Blodgett films (16), self-assembled monolayers (SAMs) (17, 18), and assemblies of triblock copolymers (19). However, there have been no reports on the preparation of free-standing nanoscale sheets from biocompatible and biodegradable materials only. The nanosheets would be a candidate as a new injectable biomaterial in drug delivery systems.

Organosilane SAMs have been widely applied to control physical and chemical properties of the surfaces of glass, quartz, SiO_2/Si wafers, or silica particles (20). Furthermore, they are excellent tools to study the immobilization of proteins such as redox proteins (21), enzymes (22), and immunoglobulins using covalent bonds or non-covalent bonds such as ionic or hydrogen bonds, van der Waals attraction, and hydrophobic interaction with the various terminal groups of SAMs. Generally, it is easy to construct patterned SAMs with uniform sizes and shapes on silicon oxide or gold substrates using conventional photolithography processes (23). This approach was used for the electrochemical analysis of

proteins immobilized by adsorption on the substrates. ~~This approach was used for the electrochemical analysis of proteins immobilized by adsorption on the substrates.~~

Here, we proposed a novel method to prepare a free-standing biocompatible nanosheet having hetero-surfaces. We used a patterned hydrophobic octadecyltrimethoxysilane-SAM (ODS-SAM) on silicon oxide to prepare nanosheets of uniform sizes and shapes. Furthermore, we modified the surface of the nanosheet with fluorescent latex beads as a model material to prove the fabrication of a nanosheet with hetero-surfaces.

MATERIALS AND METHODS

Reagents

P-type Si (100) wafers (below 0.02 Ω cm) covered with thermally grown silicon oxide (approximately 30 nm) was purchased from KST World, Co. (Fukui, Japan). n-Octadecyltrimethoxysilane (ODS, 97%) was purchased from Gelest, Inc. (Morrisville, PA). Succinimidyl 6-[3'-(2-pyridyldithio) propionamido] hexanoate (LC-SPDP) and *N*-(ε-maleimidocaproyl) succinimide ester (EMCS) were purchased from Pierce Biotechnology, Inc. (Rockford, IL). Dithiothreitol (DTT) and copper sulfate pentahydrate were purchased from Wako Pure Chemical Industries, Ltd. (Osaka, Japan). 5, (6)-Tetramethylrhodamine isothiocyanate (TRITC) and 7-chloro-4-nitrobenzo-2-oxa-1,3-diazole (NBD) were purchased from Invitrogen, Co. (Carlsbad, CA). Sephadex G25 for gel permeation chromatography (GPC) was purchased from GE Healthcare UK, Ltd. (Buckinghamshire, England). Latex beads (Polybead^{TM}, 100 nm ϕ) were purchased from Polysciences, Inc. (Warrington, PA). Recombinant human serum albumin (rHSA, 250 mg/mL) was kindly donated by Oxgenix Co., Ltd. (Tokyo, Japan).

SAM preparation

Silicon wafers were treated with SPM (96 % H_2SO_4: 30 % H_2O_2 = 4:1 (v/v)) at 120 °C followed by rinsing with distilled water. The resulting wafers were placed in a 20 mL teflon vial containing a glass cup filled with 200 μL ODS liquid. The vials were sealed with a cap and then heated for 8 hrs at a constant temperature of 110 °C in a dry room to prepare a hydrophobic ODS-SAM on the silicon oxide (24).

Patterning processes

The patterned ODS-SAM having hydrophobic octadecyl regions and hydrophilic silicon oxide regions on the substrate was prepared by a conventional photolithography process. The ODS-SAM on the silicon oxide was covered with a photoresist (OFPR-800 500 cP, Tokyo Ohka Kogyo, Co. Ltd., Kanagawa, Japan), and was irradiated with a 350 nm UV lamp (MA-10, Mikasa Ltd., Tokyo, Japan) using a photomask (size: 1 cm x 1 cm, patterning; rectangle (10 μm x 30 μm), Topic Co., Ltd., Saitama, Japan). After developing (NMD-3), the substrate was exposed to oxygen plasma (Plasma Reactor PR301, Yamato Scientific Co. Ltd., Tokyo, Japan) at an input power of 200 W and an oxygen flow rate of 80 sccm for removal of ODS. The photoresist was removed by acetone washing to obtain the patterned ODS-SAM.

Contact angle measurements

A 3 μL drop of distilled water was placed directly onto the ODS-SAM with a micro-pipette before and after rHSA adsorption, or after the addition of surfactant as described below. The liquid drops were observed with an optical microscope with 5x magnification. All water contact angles represented the mean ± standard deviation of the five measurement values.

Chemical modification of rHSA with thiol groups

An rHSA solution (250 mg/mL) was diluted to 50 mg/mL with a phosphate buffer solution (pH 7.4). A 50 mM solution of LC-SPDP in DMSO (150 μL) was added to the rHSA solution (1 mL), and the solution was incubated for 20 min at r.t.. To the rHSA solution, a 10 mM TRITC phosphate buffer solution (112.5 μL, pH 7.4) was then added and incubated for 20 min at r.t.. The unreacted LC-SPDP (precipitated), TRITC, and the by-products were separated by centrifugation and then by GPC with an acetate buffer (pH 5.0) to obtain a pyridyl disulfide-bearing rHSA (PD-rHSA). DTT (Final concentration (f.c.) 20 mM) was added to the PD-rHSA solution to reduce the PD group to a SH group. The unreacted DTT and the by-products were separated by GPC with an acetate buffer (pH 5.0), and the fractions of TRITC-labeled thiol-introduced rHSA (TRITC-labeled SH-rHSA) were collected. The

number of the SH groups conjugated to one rHSA molecule was determined by the quantification of the 2-thiopyridone (2-TP) at 343 nm that was liberated by the addition of DTT.

Preparation of rHSA-nanosheets

As shown in Fig. 1, the substrate of the patterned ODS-SAM was immersed into an acetate buffer solution (pH 5.0) of the TRITC-labeled SH-rHSA at a concentration of 1 μg/mL for 1 hr at r.t., and washed with an acetate buffer solution to remove the non-adsorbed SH-rHSA. The substrate was immersed into an acetate buffer solution containing copper ion (II) as a catalyst (25) at a concentration of 1 μM for 12 hrs at r.t.. The series of adsorption, cross-linking and washing processes were repeated three times. The substrate was immersed into a 1% (v/v) deca(oxyethylene) dodecyl ether ($C_{12}E_{10}$) solution at r.t. for 6 hrs to obtain a free-standing rHSA-nanosheet suspension by releasing the rHSA-nanosheets from the substrate. We observed the resulting rHSA-nanosheets using an epifluorescence microscope (ECLIPS TE300, Nikon Co., Tokyo, Japan) equipped with a CCD camera, a confocal laser scanning microscope (LSM 510, Zeiss, Nikon Co., Tokyo, Japan), and an atomic force microscope (AFM) at a tapping mode with a MFP-3D-BIO (Asylum Research, Co., Santa Barbara, CA).

Conjugation of NBD-labeled latex beads to the surface of rHSA-nanosheets

Latex beads (ϕ 100 nm) were mixed with an rHSA solution (50 mg/mL) and incubated at r.t. for 2 hrs to coat the surface of the latex bead with rHSA. After the separation of the free rHSA by ultracentrifugation (100,000*g*, 10 min, 4 °C, twice), the rHSA-coated latex beads (rHSA-latex beads) were dispersed in a phosphate buffer solution (pH 7.4). The amount of rHSA adsorbed on the surface of the latex bead was analyzed by a microBCA kit (Pierce Biotechnology, Inc. (Rockford, IL). A solution of LC-SPDP in DMSO (2 eq. mol with respect to the rHSA adsorbed on the surface of the latex bead) was added to the suspension of the rHSA-latex beads and incubated for 20 min at r.t. The solution of NBD in DMSO (2 eq. mol with respect to rHSA on the surface of the latex bead) was added to the suspension and incubated for 20 min at r.t.. A DTT treatment (f.c. 20 mM) was carried out to reduce the PD

groups to SH groups. The unreacted DTT and by-products were separated by GPC, and the NBD-labeled thiol-bearing latex beads (SH-(NBD)latex beads) were collected.

On the other hand, the substrate of the TRITC-labeled rHSA-nanosheets was immersed in a phosphate buffer, and a DMSO solution of EMCS was added to the substrate and incubated for 20 min at r.t. to introduce maleimido groups on the nanosheet. The unreacted EMCS and by-products were washed with a phosphate buffer, and the maleimido-bearing rHSA-nanosheets were obtained.

Finally, the SH-(NBD)latex beads were added to the maleimido-bearing rHSA-nanosheets, and incubated for 2 hrs at r.t.. The unreacted SH-(NBD)latex beads and by-products were washed with a phosphate buffer, and the rHSA-nanosheets, of which the obverse side was modified with the NBD-labeled latex beads, were observed using a confocal laser scanning microscope (LSM 510) and a Hitachi S-4500 field emission scanning electron microscope (SEM).

RESULTS

Water contact angle

The water contact angle of the substrate, which was coated with ODS-SAM, was estimated to be 83 $\pm$ 1° as listed in Table 1. When the ODS-SAM-coated substrate was immersed into a phosphate buffer solution (pH 7.4) of rHSA at a concentration of 100 μg/mL, the water contact angle did not change (80 $\pm$ 2°). However, when the substrate was immersed in an acetate buffer solution (pH 5.0) of rHSA, the angle was significantly decreased to 67 $\pm$ 1°. The angle was restored to 82 $\pm$ 1° when the rHSA-treated substrate was immersed into a 1% (v/v) solution of $C_{12}E_{10}$ for 1 hr. Therefore, we confirmed that rHSA molecules were adsorbed on the ODS-SAM at pH 5.0, and the adsorbed rHSA molecules were detached from the substrate by the surfactant treatment.

Preparation of rHSA-nanosheets

We could not analyze the cross-linking ratio of the SH-rHSA molecules adsorbed on the ODS-SAM from quantification of the unreacted SH groups of the rHSA because the amount of the adsorbed rHSA was below the detection limit. We explored the cross-linking of

the SH-rHSA in an aqueous solution in order to determine the extent of cross-linking of the SH-rHSA on the ODS-SAM. We determined the number of SH groups bound to one rHSA molecule for mixtures of LC-SPDP and rHSA at 5, 7 and 10 mol/mol (mole equivalent of the rHSA concentration) ratios of LC-SPDP to rHSA. Based on the quantification of the 2-TP liberated by the addition of DTT, the number of SH groups bound to one rHSA molecule was estimated to be approximately 2.9 ± 0.8, 4.7 ± 1.1, and 7.4 ± 1.2 molecules, respectively. We oxidized the SH-rHSA molecules in the presence of copper ion (II) at r.t. and measured the degree of reaction by HPLC with a TSK-GEL G4000SW_{XL} column, by measuring the absorbance of the column effluent at 220 nm, which was attributed to the absorption of the amide linkage of rHSA. At pH 5.0, the three kinds of SH-rHSA having different numbers of SH groups were cross-linked, and the percentage of the peak area of the void fraction to the total peak, which corresponded to the amount of the cross-linked rHSA with a molecular weight of >670 kDa based on the elution time of thyroglobulin as a marker protein, was increased to 64, 75, and 96 % with the increasing number of the SH groups bound to one rHSA molecule. All reactions finished within 12 hrs. On the other hand, the three kinds of SH-rHSA were hardly cross-linked in the absence of copper ion (II) at pH 5.0 or in the presence of copper ion (II) at pH 7.4. Based on the above results, we decided that SH-rHSA molecules with 7.4 ± 1.2 SH groups bound to one rHSA molecule were to be cross-linked on the patterned ODS-SAM at pH 5.0 for 12 hrs in the presence of 1 μM copper ion (II).

Next, we explored the adsorption of SH-rHSA on the rectangle patterned ODS-SAM regions. When the substrate of the patterned ODS-SAM was immersed in an acetate buffer solution (pH 5.0) of the TRITC-labeled SH-rHSA at a concentration of 1 μg/mL, the rectangular patterns (10 μm x 30μm) were completely and selectively stained by the TRITC-labeled SH-rHSA as shown in Fig. 2 (a). After removing the non-adsorbed SH-rHSA by washing with the acetate buffer solution, we cross-linked the SH-rHSA molecules adsorbed on the patterned ODS-SAM in the above conditions, and immersed the substrate in a 1% $C_{12}E_{10}$ solution at r.t. for 6 hrs to detach the rectangles from the substrate. Next, we dropped the $C_{12}E_{10}$ solution containing the rectangular sheets onto a glass plate, and observed the surface of the plate using a confocal laser scanning microscopy. There were abundant rectangular rHSA-nanosheets in various conformations; in particular, the bent form of the